Available online at www.pelagiaresearchlibrary.com

Pelagia Research Library

Advances in Applied Science Research, 2012, 3 (4):2090-2102

ISSN: 0976-8610
CODEN (USA): AASRFC

Study of hygrothermal transfer through porous clay tubes application to the cooling of water volume in the sahelian zone

S. Kam[a], M. Zongo[b], B. Dianda[a], A. Konfé[a], D. J. Bathiebo[a] and L. Aurélien[c]

[a]Renewable Thermal Energy Laboratories, Physics department, University of Ouagadougou, 03 BP 7021 Ouagadougou 03 Burkina Faso
[b]UFR/SEA, Physics Department, University of Ouagadougou, 03 BP 7021 Ouagadougou 03 Burkina Faso
[c]Department of Engineering, Liquid-air company, 75 Quai d'Orsay,75321, Paris Cedex 07.

SUMMARY

After conducting studies on hygrothermal transfer in porous terracotta tube, we present here a study of the cooling of a water reserve in hot, dry climate. This water is contained in a parallelipedic enclosure, through which porous tubes placed in staggered rows are subjected to a forced convection of hot dry air. The aspect ratio ($F = D / L \approx 0.32$) allows to neglect the longitudinal variations of the thermo physical properties of air. The theoretical model is based on the Darcy equation for the fluid through the porous material, the Laplace equation relating to pressure and the equation of heat in polar coordinates. An improved computer code that takes into account the variation of heat transfer coefficients at each time step allows better simulations. The code of calculation enables to identify areas of intrinsic permeability favorable for continuous low evaporation without drying of the water film and this computer code enables to describe the hygrothermal transfer.

Keywords: cold, evaporation, forced convection, hot, dry air.

NOMENCLATURE

C	Compactness C ($m^2 . m^{-3}$)
Cp	specific heat at constant pressure ($J.kg^{-1}K^{-1}$)
D	mass diffusivity ($m^2 s^{-1}$)
Di	inner diameter (m)
Do	outer diameter (m)
G	acceleration of gravity ($m.s^{-2}$)
Gr	Grashof number
H	height (m)
ha	heat transfer coefficient of the air ($W.m^{-2}.K^{-1}$)
he	heat transfer coefficient of water ($W.m^{-2}.K^{-1}$)
hm	mass transfer coefficient ($m.s^{-1}$)
K	Hydraulic conductivity ($m.s^{-1}$)
Kp	Intrinsic permeability (m^2)
L	tube length (m)
Lv (p)	latent heat of evaporation at the temperature T ($J.kg^{-1}$)
Me	mass of water (kg)
m	mass flow rate ($kg.s^{-1}$)
Nu	average Nusselt number
P	pressure (Pa)
Pr	Prandtl number (υ / α)
R	radius of the tube (m)

Re Reynolds number Re
Rv perfect gas constant on the water vapor (J.kg.K^{-1}.mole^{-1})
Sc Schmidt number
S1 surface of the tube (m^2)
Se outer surface of the tube (m^2)
Sh Sherwood number Sh
T temperature (° C)
U radial velocity (m.s^{-1})
V Tangential speed V (m.s^{-1})
V_T total water volume (m^3)

Greek symbols

αm thermal diffusivity (m^2.s^{-1})
ε porosity
θ angular coordinate
λ thermal conductivity (W.m^{-1}K^{-1})
μ dynamic viscosity (kg.m^{-1}s^{-1})
ρ density (kg.m^{-3})
υ kinematic viscosity (m^2.s^{-1})

Indices

a air
d diameter
e water
f Interface
i Internal
o external
s saturation

INTRODUCTION

Among the very simple processes of cooling we can list the phenomenon of evaporation of water film appearing on a porous surface licked by a flow of hot dry air, [1], [2], [3], [4], [5].

The traditional knowledge of sub-Saharan Africa's potters, in the Sahelian zone, allows the manufacture of slightly porous earthenware, which refreshes stored water, by evaporation of the water film deposited on the walls.

In Sahelian countries, the differences between the dry bulb temperature and wet bulb temperature may be above 15 degrees (Figure 1).

The hot, dry air, available for nine months of the year is then a favorable factor in our process of evaporative cooling. The reserve of resulting cold water in contact with an aluminum pan containing food, helps preserve it longer.

The transfer of mass and heat during this evaporation is often described by the following empirical expressions:

$$Nu = a\,\mathrm{Pr}^m\,\mathrm{Re}^n, \quad Sh = a_1 Sc^{m_1}\,\mathrm{Re}^{n_1} \qquad (1a, b)$$

in which the coefficients a, a1, m, m1, n, n1 depend on the properties of the fluid and on the Reynolds number. Mass and heat transfer between the interface of a saturated porous medium, subjected to evaporation and an external gas flow has been theoretically analyzed by Morgan et al. [6].

The theory of boundary layers has been applied to the evaporation of the liquid contained in the porous material. The resulting equations enable to do without the number of Gukhman by using relations of type (1).

Kondjoyan et al. [7] developed a method based on psychrometrics for simultaneous measures for mass and heat transfer coefficients by forced convection between air and a wet surface. This method that was tested on tubes allows the easy evaluation of the transfer coefficients.

Recently, Prabal et al. [8], have developed a computer code (CFD), simulating in a laminar mode the convective mass and heat transfer in three dimensions.

This code is applied between a wet surface and a current of air flowing horizontally in a rectangular channel, in order to validate their experimental data. Conrad et al. [9]. (A thin water layer is based on the lower surface of the channel). The numerical data obtained are consistent with those obtained experimentally (with negligible uncertainties of measurements). The effect of gravitational forces has been negligible. In this study the average numbers of Nusselt and Sherwood are calculated by:

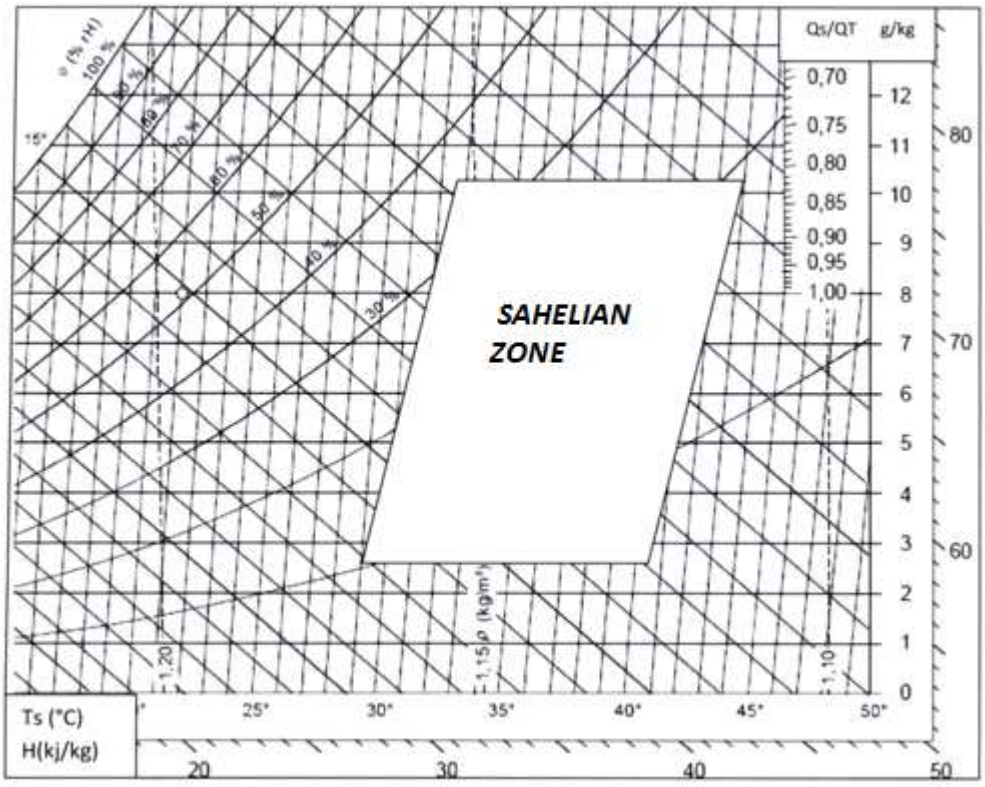

Figure 1: Zone of the psychrometric diagram in Sahelian climate

; . (2 a, b)

$$\overline{Nu} = \int_0^z \frac{\left.\frac{-\partial T}{\partial y}\right|_{y=0}}{\Delta T} dz \qquad \overline{Sh} = \int_0^z \frac{\left.\frac{-\partial C}{\partial y}\right|_{y=0}}{\Delta C} dz$$

(Z is the coordinate in the direction of air flow and y is in the vertical)

Studies of L. Berman [10] on determining the ratio Sh / Nu for different flow patterns show that for water temperatures between 20 and 50 ° C, the ratio remains substantially constant,

very close to 1, $\frac{Sh}{Nu} = 1.06$

Over a long period, in a variable process, we cannot use average coefficients to properly transcribe the coupling between external transfer in the boundary layer and internal transfer in the porous medium. These coefficients are then recomputed with each step of time.

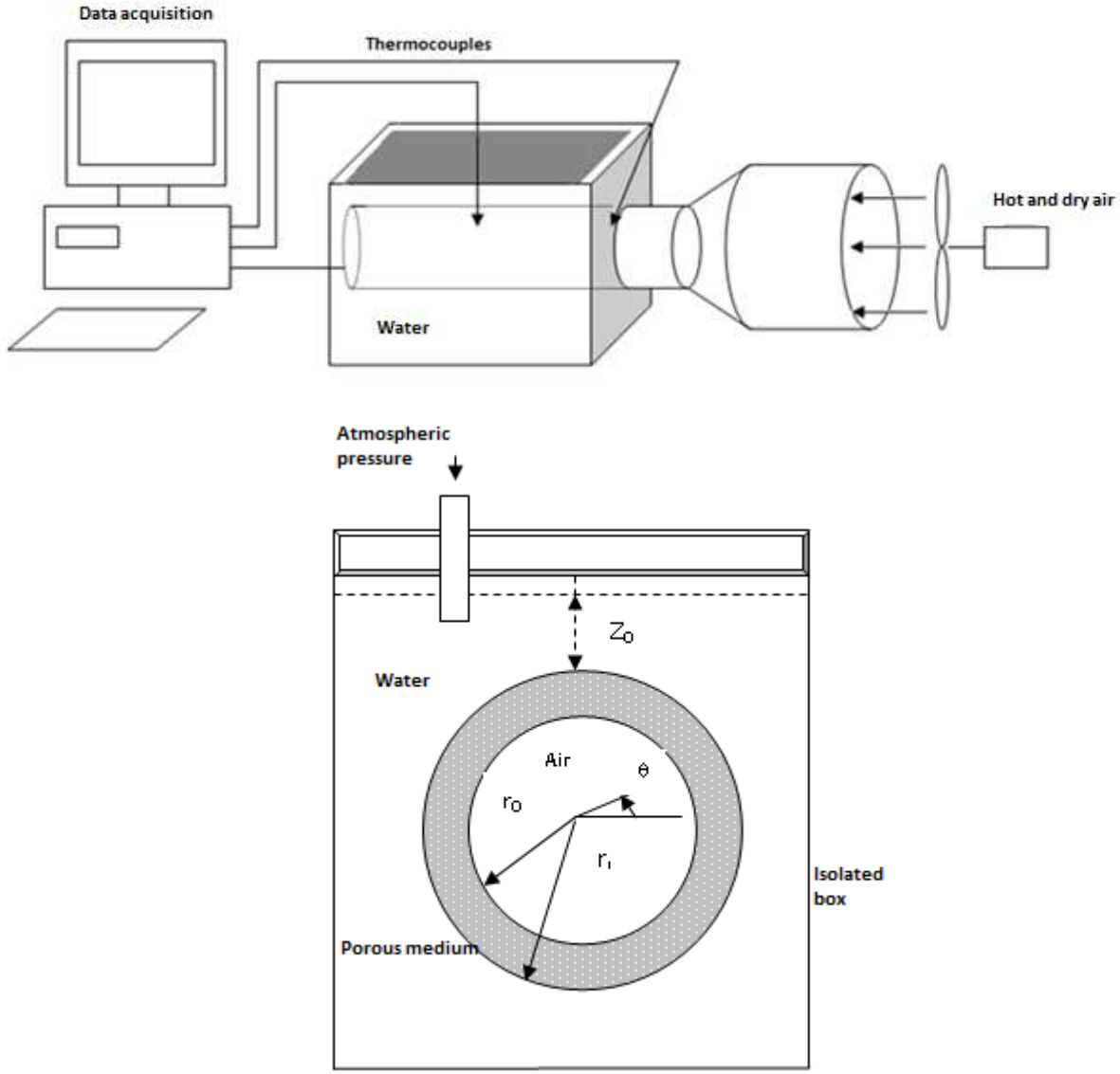

Figure 2: Diagrams of the studied system

To validate the computational code adopted, we built a small heat exchanger, a parallelepiped shape, containing a volume of water with a porous tube crossing it, through which the hot, dry air can circulate. The aspect ratio F, (F = D / L) is selected so that the longitudinal variations of the thermo physical properties of the air are negligible, in particular (F <0.32). The air then gives its sensible heat to the film carried by the wall which transfers to it its latent heat by evaporation.

Figure 2 shows the diagram of the studied system. In this code, is recalculated at each time step, the coefficients of mass and heat transfer that is reintroduced into the system of equations.

The thermo-physical properties of this clay had been in major part, determined at the National School of Industrial Ceramics of Limoges, in collaboration with The Group for the Study of Heterogeneous Materials (GEMH) (see Appendix and [2]).

2. Formulation of the problem

We consider a porous tube initially dry (Do = 8cm, Di = 6 cm), a porosity equal to 0.323, whose inner wall surface is in contact with the flow of hot dry air and whose outer surface is immersed in a container of water with a 18cm square section of side. It has a small agitator which homogenizes the temperature of the water. We can then define the compactness of our system by the ratio C = (Se / V_T) = 7.75.

The outer surface of the wall is then subjected to a variable hydraulic load $P(r,\theta)$. The capillary invasion is made when the internal surface becomes saturated. There is then a very slow phenomenon of percolation. Measurements carried on different terracotta by CTTB, 1998 [11] and B. Perrin et al. [12], show that the percolation phenomenon occurs only when the water film is approximately 163 g of water / m2 of wall. It is at this moment that we send the hot dry air in the canal. Subsequently, there occurs a phenomenon of competition between on the one hand, the water coming to the film through the material and on the other hand, the flow evaporated in the air. Indeed the hot dry air gives up its sensible heat to the film of water which transfers to it its latent heat.

2.1 Assumptions:

- The porous material is homogeneous and constantly saturated with water,
- Density and fluid viscosity are assumed to be constant,
- The porous medium is isotropic and permeability K_p is constant in all directions
- At each point of the porous medium the solid matrix is in thermal equilibrium with the fluid filling the pores.
- The porous medium can be treated as a continuum resulting from the simultaneous presence of two phases (solid and liquid in our case). It is then modeled by a fictitious continuous medium, homogeneous and isotropic. The physicochemical characteristics of this medium $(\lambda_{m,}(\rho Cp)_m..)$ can be obtained by composition laws.

- The local Reynolds number $Re = \frac{u.K_p^{1/2}}{\upsilon}$ is very low (<10), speed filtration then obeys Darcy's law: Bejan, [13]. Most of the research efforts [14], [15] concerned free convection using Darcy's law, which states the volume-averaged velocity is proportional to the pressure gradient.

The flow of water passing through the wall of the porous tube is negligible compared to the water body of the container which is assumed to be constant.

The pressure of saturating vapor is related to the temperature T of the water film by means of Bertrand's formula:

$$P_{vs} = 101300.[10^{(17.443-\frac{2795}{T}-3.868\log_{10}(T))}] \quad (3)$$

2.2 The transfer equations

We set

$$\lambda_m = \varepsilon\lambda_e + (1-\varepsilon)\lambda_s ;\ \alpha_m = \frac{\lambda_m}{(\rho Cp)_e} ;\ \sigma = \frac{\varepsilon\rho_e Cp_e + (1-\varepsilon)\rho_s Cp_s}{\rho_e Cp_e} ;\ K = K_p/\mu$$

The equation of conservation of mass in a saturated porous medium leads to solving the Laplace equation for pressure

$$\frac{\partial^2 P}{\partial r^2} + \frac{1}{r}\frac{\partial P}{\partial r} + \frac{1}{r^2}\frac{\partial^2 P}{\partial \theta^2} = 0 \quad (4)$$

Equations of Motion:

$$U = -K(\frac{\partial P}{\partial r} + \rho g_r) \quad \text{with} \quad g_r = g.\sin\theta \quad (5)$$

$$V = -K(\frac{\partial P}{r\partial \theta} + \rho g_\theta) \quad \text{with} \quad g_\theta = g.\cos\theta \quad (6)$$

Heat equation in the porous medium

$$\sigma\frac{\partial T}{\partial t} + U\frac{\partial T}{\partial r} + V\frac{\partial T}{r\partial \theta} = \alpha_m(\frac{\partial^2 T}{\partial r^2} + \frac{1}{r}\frac{\partial T}{\partial r} + \frac{1}{r^2}\frac{\partial^2 T}{\partial \theta^2}) = 0 \quad (7)$$

The average temperature of the water is calculated from the following equation:

$$M_e Cp_e \frac{\partial \overline{T_e}}{\partial t} = \overline{Nu} \frac{\lambda_e}{d_e} S_o (T - \overline{T_e}) \quad (8)$$

2.3 Calculation of mass and heat transfer coefficients:

The average velocity of the air in the duct is approximately 1 $m.s^{-1}$. We obtain Reynolds numbers that are higher than 2300, so that we are dealing with a turbulent flow. We then use the correlation of Gilliland [16].

$$Sh = 0{,}023.Re_d^{0,83}.Sc^{0,33}; \qquad h_m = \frac{Sh.D}{d_i} \quad (9a, b)$$

The coefficient of convective heat exchange between the air and the wall is evaluated from the correlation of Colburn [17], in turbulent flow:

$$Nu_a = 0{,}023.Re_d^{0,80}.Pr^{0,83}; \quad h_a = \frac{Nu.\lambda_a}{d_i} \quad (10a, b)$$

The coefficient of heat transfer between the wall and the water is obtained from the following correlation:

$$\overline{Nu}_e = 0{,}57.Gr^{0,25}.Pr^{0,83}; \quad h_e = \frac{Nu.\lambda_e}{d_e} \quad (11)$$

Wherein the Grashof number is calculated from the average temperature of the wall

$$\overline{T(r_1, \theta)} = \frac{1}{\pi} \int_0^{\pi} T(r_1, \theta) d\theta \quad (12)$$

Initial conditions

$$t = 0; \; T_f = T = T_e = T_0 \quad (13)$$

Boundary conditions

At the level of (r_0, θ) :

$$-\lambda_m \left. \frac{\partial T}{\partial r} \right|_{r_0, \theta} = h_a S_i (\overline{T_f} - T_a) - \dot{m}.Lv_{(\overline{T_f})}; \quad \text{avec} \quad \dot{m} = \frac{h_m S_i}{R_v \overline{T}_f} (P_{vs(T_f)} - P_{va}); \quad (14)$$

$$P = P_0 \quad (15)$$

At the level of (r_1, θ) :

$$-\lambda_m \left. \frac{\partial T}{\partial r} \right|_{r_1, \theta} = h_e (T_e - T) \quad (16)$$

$$P = P_0 + \rho g (z_0 + r_1 (1 - \sin \theta)) \quad (17)$$

2.4 Numerical solution

Equations (4) (7) (8) are discredized by using an implicit scheme at central differences. The density of the fluid is constant, the speeds are calculated from solutions of the Laplace equation relating to pressure, and then introduced into the equation of heat.

The systems of algebraic equations (4), (15), (17) on the one hand and (7), (14), (16) on the other hand are solved by using the Gauss algorithm.

We construct in polar coordinates (r,θ) , a regular mesh of 120 nodes according to the coordinate r and 32 knots according to coordinate θ with $r = i\Delta r$ and $\theta = j\Delta\theta$ where i and j are integers, (Figure 3).

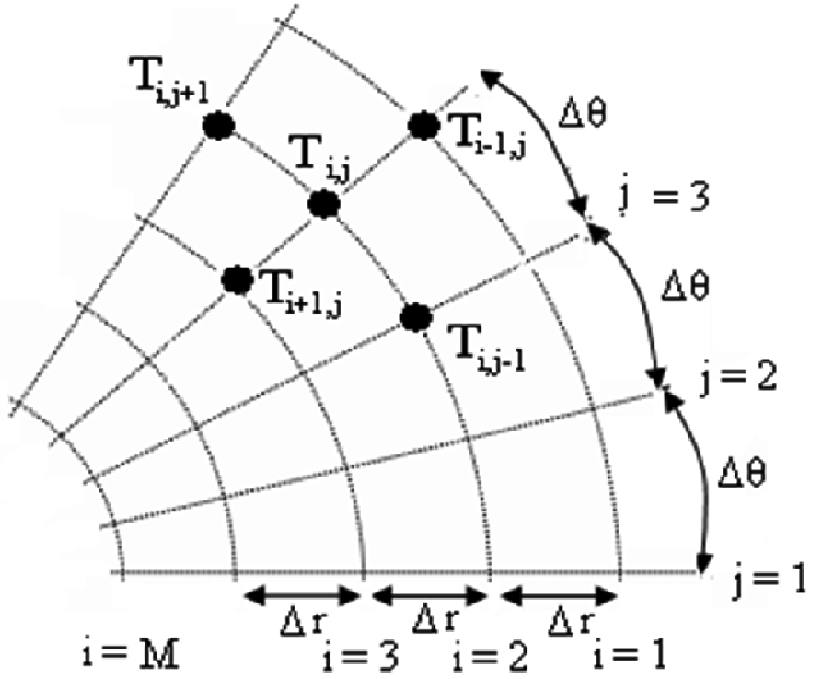

Figure 3: Diagram of the grid used

Pressure $P(r,\theta)$ and temperature $T(r,\theta)$ can be written at any point M:

$$P(r,\theta)\big|_M = P(i\Delta r, j\Delta\theta) = P(i,j)$$

$$T(r,\theta)\big|_M = T(i\Delta r, j\Delta\theta) = T(i,j)$$

The second derivatives are discretized as follows:

$$\left.\frac{\partial^2 T}{\partial r^2}\right|_M = \left.\frac{\partial^2 T}{\partial r^2}\right|_{i,j} = \frac{T_{i-1,j} - 2T_{i,j} + T_{i+1,j}}{\Delta r^2} + 0(\Delta r^2)$$

$$\left.\frac{\partial^2 T}{\partial \theta^2}\right|_M = \left.\frac{\partial^2 T}{\partial \theta^2}\right|_{i,j} = \frac{T_{i,j-1} - 2T_{i,j} + T_{i,j+1}}{\Delta\theta^2} + 0(\Delta\theta^2)$$

For the Laplace equation, we get:

$$\frac{P_{i-1,j} - 2P_{i,j} + P_{i+1,j}}{(\Delta r)^2} + \frac{1}{i\Delta r}.\frac{P_{i+1,j} - P_{i-1,j}}{2\Delta r} + \frac{1}{i^2(\Delta r)^2}\frac{P_{i,j-1} - 2P_{i,j} + P_{i,j+1}}{(\Delta\theta)^2} = 0$$

After grouping the various terms, we obtain:

$$\frac{1}{(\Delta r)^2}\left(\left(1 - \frac{1}{2.i}\right)P_{i-1,j} - 2.P_{i,j} + \left(1 + \frac{1}{2.i}\right).P_{i+1,j}\right) + \frac{1}{i^2.(\Delta r.\Delta\theta)^2}.(P_{i,j-1} - 2P_{i,j} + P_{i,j+1}) = 0$$

The velocities are then calculated by the following formulas:

$$U_{i,j} = -K\left[\left(\frac{1}{2\Delta r}\right).(P_{i+1,j} - P_{i-1,j}) - \rho.g.\sin((j-1).\Delta\theta)\right]$$

$$V_{i,j} = -K\left[\left(\frac{1}{r_1 - (i-1).\Delta r}\right).\frac{P_{i,j+1} - P_{i,j-1}}{2.\Delta\theta} - \rho.g.\cos((j-1).\Delta\theta)\right]$$

The heat equation:

$$T_{i-1,j}^{n+1}.\left(\Delta t(\frac{-U}{2\Delta r} - \frac{\alpha_m}{(\Delta r)^2} + \frac{\alpha_m}{2i.(\Delta r)^2})\right) + T_{i,j-1}^{n+1}.\left(\Delta t(\frac{-V}{2i.\Delta r.\Delta\theta} - \frac{\alpha_m}{(i.\Delta r.\Delta\theta)^2})\right) +$$

$$T_{i,j}^{n+1}.\left(\sigma + \Delta t(\frac{2\alpha_m}{(\Delta r)^2} + \frac{2\alpha_m}{(i.\Delta r.\Delta\theta)^2})\right) + T_{i,j+1}^{n+1}.\left(\Delta t(\frac{V}{2i.\Delta r.\Delta\theta} - \frac{\alpha_m}{(i.\Delta r.\Delta\theta)^2})\right) +$$

$$T_{i+1,j}^{n+1}.\left(\Delta t(\frac{U}{2\Delta r} - \frac{\alpha_m}{(\Delta r)^2} + \frac{\alpha_m}{2i.(\Delta r)^2})\right) + T_{i,j-1}^{n+1}.\left(\Delta t(\frac{-V}{2i.\Delta r.\Delta\theta} - \frac{\alpha_m}{(i.\Delta r.\Delta\theta)^2})\right) = \sigma T_{i,j}^{n}$$

RESULTS AND DISCUSSION

4.1 Transferred mass flow depending on the permeability of the material

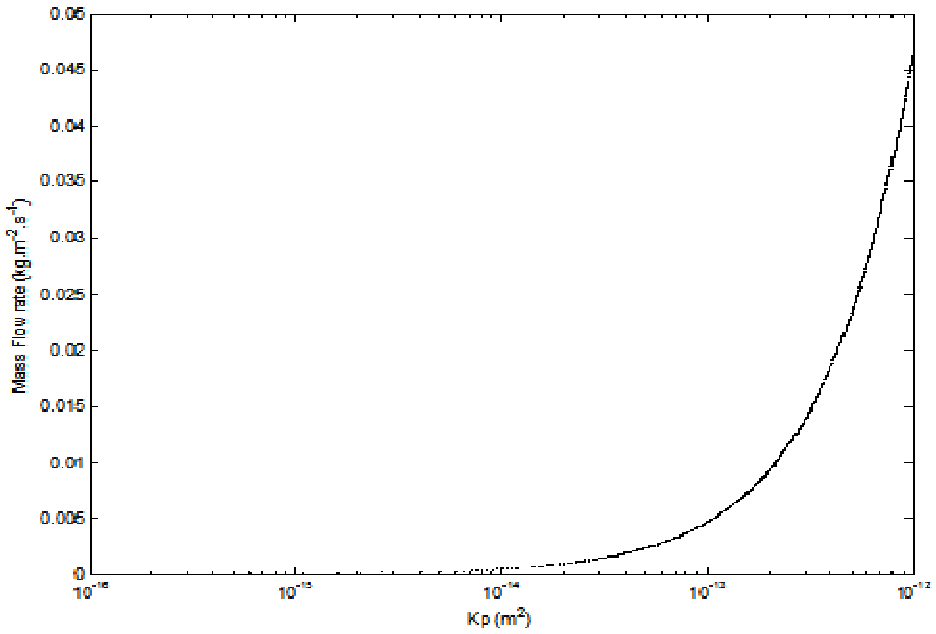

Figure 4: Flow of liquid produced on the level of the internal surface of the tube in function of permeability, in a controlled environment: a=30C, RH = 30%, Re = 3822

Figure 4 gives an order of magnitude of mass flows through the wall. Those latter grow exponentially when the intrinsic permeability is represented on a logarithmic scale. The goal is to cool as much as possible a mass of water while consuming as little as possible, the material must have such permeability so that the transferred flows are at least equal to the evaporated flux. Otherwise, it dries the tube wall and the latter is heated by heat exchange with the flow of sensitive hot dry air.

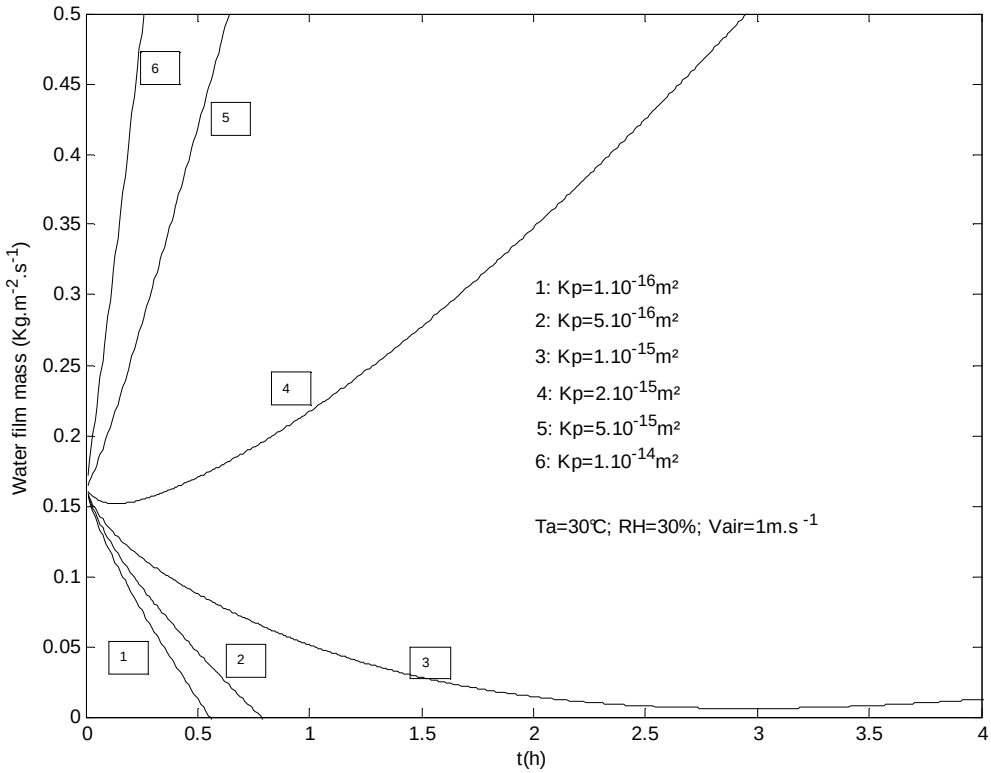

Figure 5: Evolution of the mass of water film under evaporation
Ta=30C; Hr=30%;Re = 3822;Z0 = 0.05m

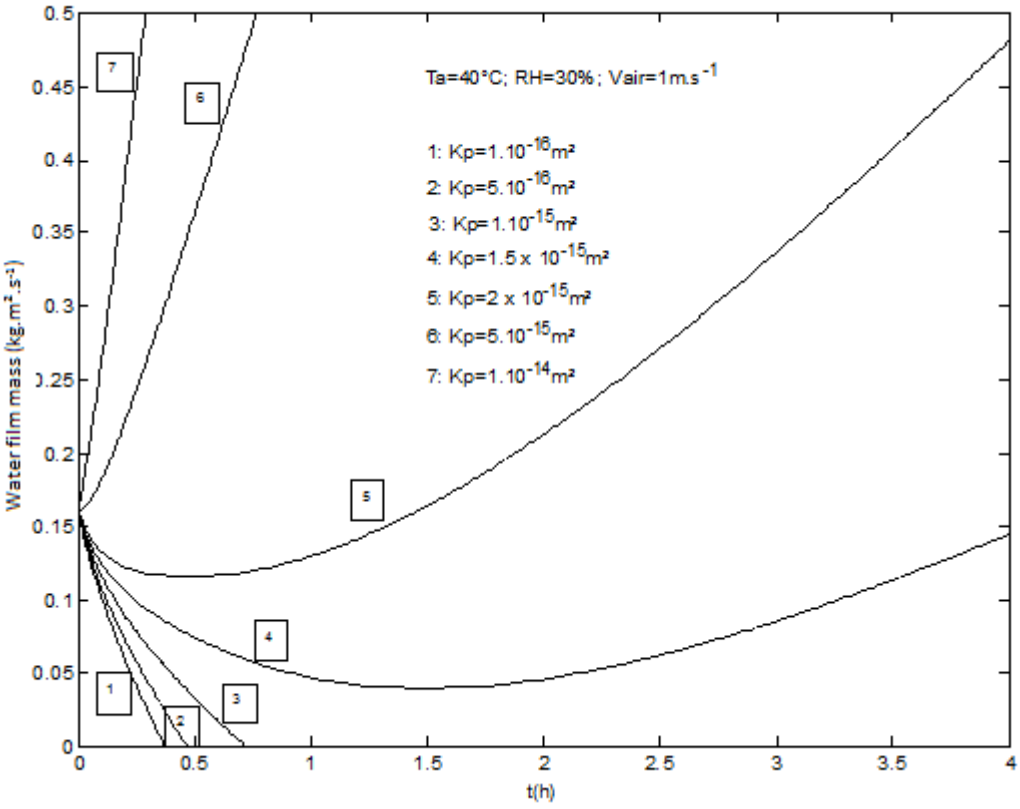

Figure 6: Evolution of the mass of water film under evaporation:
Ta=40C;Hr = 30%;Re=3822;Z0 = 0.05m.

Figures 5 and 6 show the time evolution of the resulting mass of the water film on the wall, due to the phenomenon of competition between, on the one hand, the water feeding the film through the material and on the other hand, the flow evaporated in the air. The hot dry season in Sahelian countries, is characterized by temperatures between 30 and 40 ° C with a relative humidity of the air generally less than 30%.

Figure 5 shows that for values of K_p less than10^{-15} m², the wall dries out after 30 to 45 minutes. For $K_p = 10^{-15} m^2$, the mass of liquid film decreases in the early hours and then tends to increase beyond 3 hours.
Figure 6 also shows, for evaporation at 40 ° C, a more important area of drying of the wall ($K_p \leq 10^{-15} m^2$), an area conducive to evaporation of the liquid film without drying of the wall over time $(1.5\times10^{-15} \leq K_p \leq 2\times10^{-15}) m^2$. In both scenarios we notice that for permeability greater than the previous, the mass of the water film increases very fast and this area is not therefore suitable for our problem.

The curves (2) in Figure 5 and curves (4) and (5) of Figure 6 have minima. This is due to the attenuation of the gradient of partial vapor of air-water pressure, since it cools over time and consequently causes a relative decrease of the flow evaporated compared to that which is provided.

4.2 Influence of equivalent thermal conductivity on the evolution of the temperature of the material.
Figure 7 shows the evolution of the temperature within the material over time. We note of course that the differences in temperature between the air-wall interface and the material-water interface decrease when the thermal conductivity is higher. These differences remain relatively small compared to the difference in the chosen thermal conductivity which is very high for of terracotta materials.

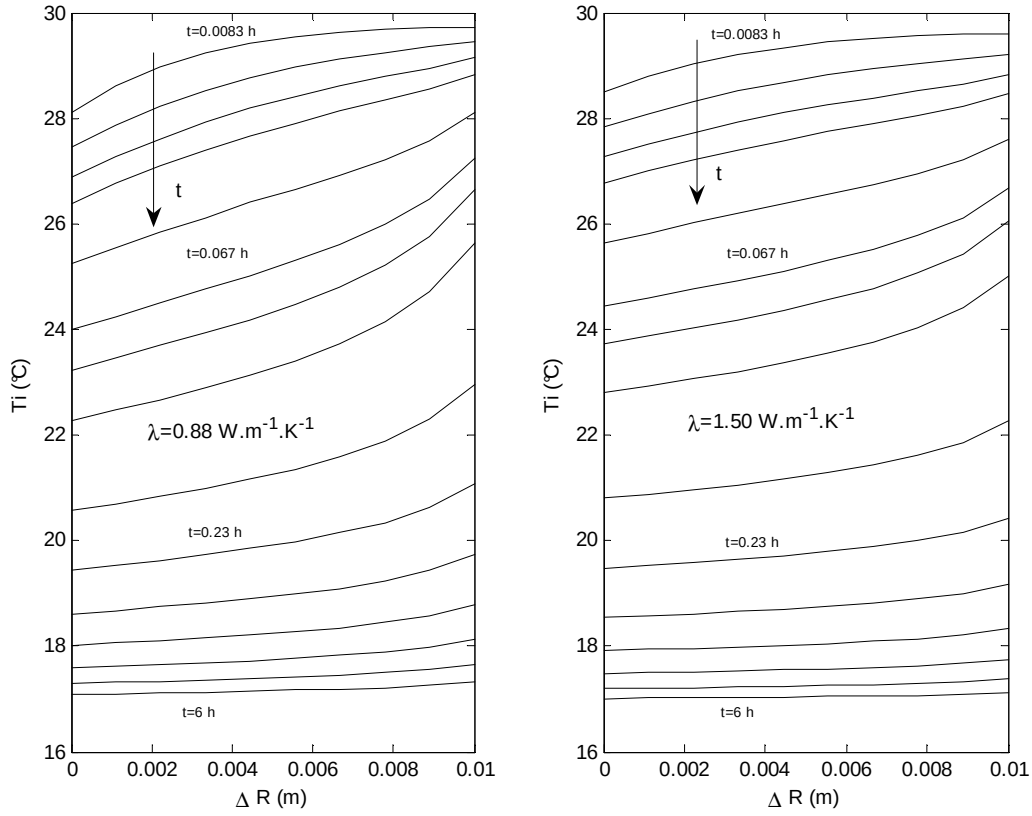

Figure 7: Change of the internal material temperature according to the thickness and time: Ta=30C;RH=30%;Re=3822;Z0 = 0.05m, Kp=2.10 $^{-5}$ m²

Temporal evolution of temperatures of film and water
The curves in Figure 8 are used to validate the computed code. The comparison of simulated and theoretical curves leads to an absolute uncertainty of about 1 ° C in temperatures. They prove that as soon as the phenomenon of

evaporation occurs, the interface cools very rapidly during the first minutes, then more slowly due to the attenuation of the gradient of partial vapor pressure of dry air, cold water film.

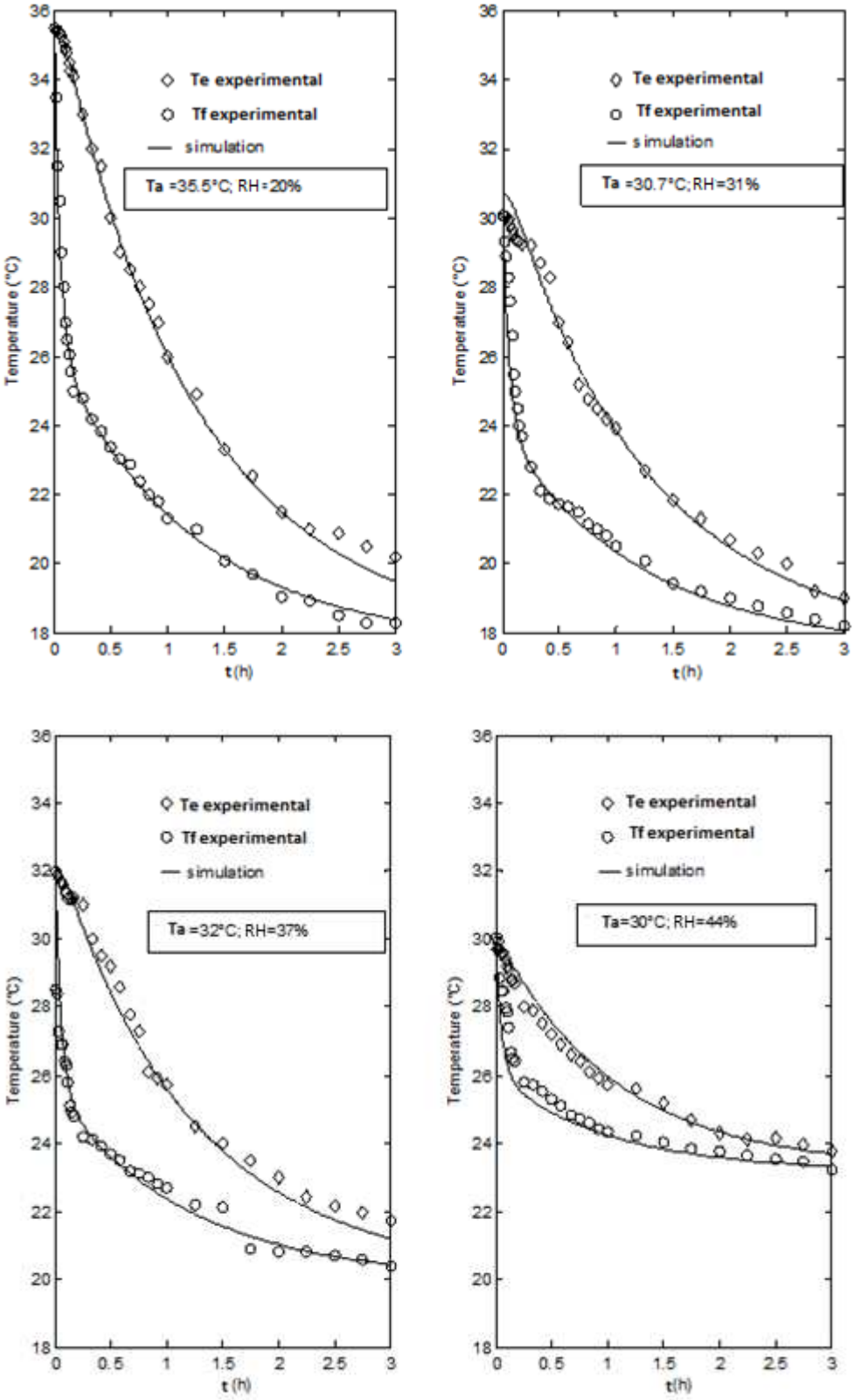

Figure 8: Validation of the computer code per comparison of the water and film temperatures, experimental and simulated, for various climatic conditions in Sahelian zone.

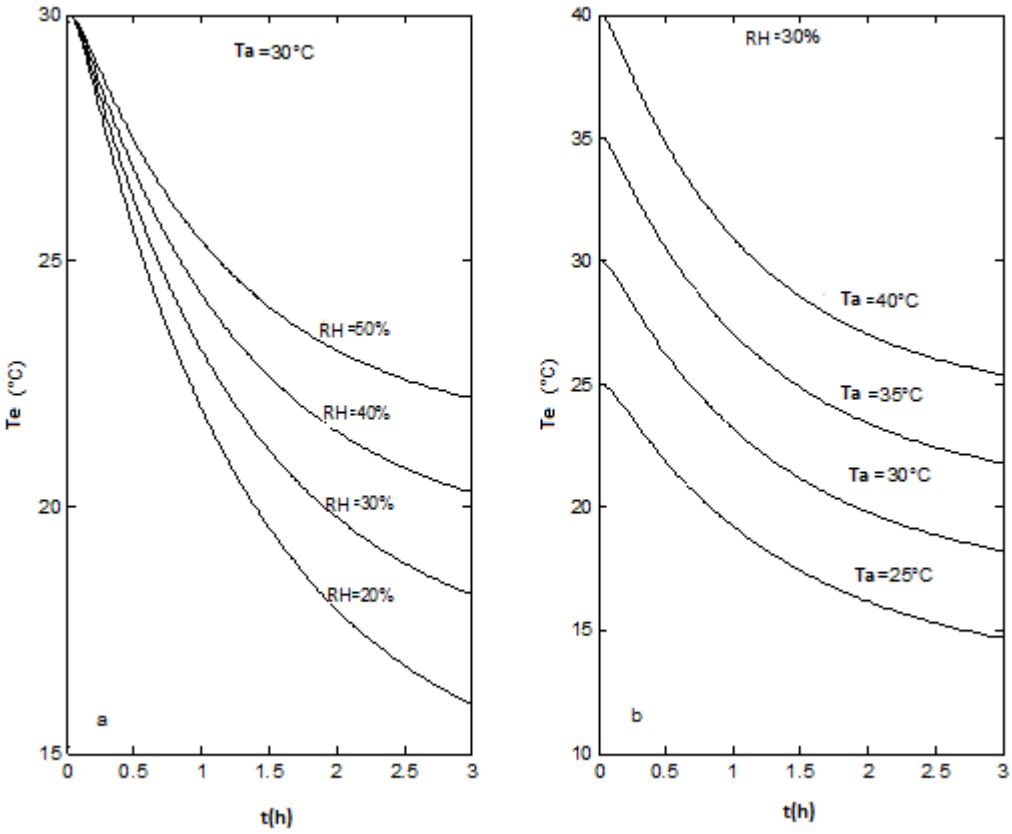

Figure 9: Simulation of the temporal evolution of the temperature of water in function of the dry temperature and the relative humidity of the air.

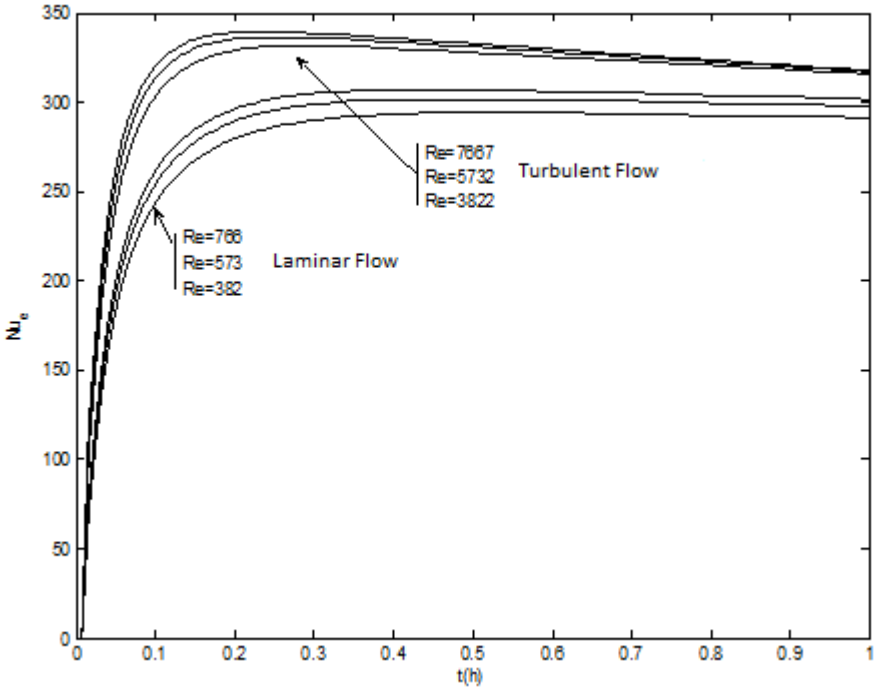

Figure 10: Variations of Nusselt number (water) according to time for different Reynolds numbers (air). Ta=30C; Hr=30%

After a few hours, the temperature of the water film on the wall approaches the wet bulb temperature. For a given dry-bulb temperature, the film temperature is lower as the relative humidity of the air is low. For a given dry temperature (Figure 9) the cooling of water is all the more so fast as the relative humidity of the air is low. The differences between room temperature and the temperature of the water are then greatest. For a fixed relative humidity of air, the water temperature is of course all the more so low as the value of the dry air temperature is low [18].

The intensification of the convection of hot, dry air inside the porous tubes results in faster cooling of the wall. Temperature differences between the outer wall of the tube and the water are then even more important. However, we notice a slight variation of Nusselt numbers characterizing the exchange between the tube wall and the water compared with the variations of Reynolds numbers obtained for air (figure 10). This means that low power ventilation is sufficient to reach temperatures close to the wet bulb temperature.

CONCLUSION

The experiments and simulations have allowed us to validate our numerical code. They indicate that one can get about fifteen Celsius degrees (15°C) below room temperature in the Sahelian zone, for a properly dimensioned system. The temperatures reached by the tank water can be considered an opportunity for the extension of the period of conservation of food products. This system needs only very low water flows to function, about 0.1($kg.m^{-2}.s^{-1}$)

Appendix: thermo physical properties of terracotta used in this work.

Volume mass ρ ($kg.m^{-3}$)	*Specific heat* $C_p(J.kg^{-1}.K^{-1})$	*Thermal conductivity dry porous material* λ_s($W.m^{-1}.K^{-1}$)	*Thermal conductivity saturated porous material* λ_e ($W.m^{-1}.K^{-1}$)	*intrinsic Permeability* $K_p(m^2)$	*Porosity* ϵ
2300	850	0.3	0.9	$1.8.10^{-15}$	32.3%

They also provide a glimpse for another application for space cooling. Indeed, when providing this system with longer porous tubes, (we extend the length of transfer between hot, dry air and wet wall), it leads to the production of cold and humid air. This aspect presents an obvious interest in hot and dry climate.

Acknowledgments
The authors thank the founding of the Company "AIR - LIQUID" for their support.

REFERENCES

[1] Kam S, Bathiébo DJ, Dissa AO, Traoré K, and Aurélien L, *International Journal of Ambient Energy*, **2008**, 29, 3, 115.
[2] Kam S, Bathiébo DJ, Zerbo L, Soro J, Traoré K, Blanchart P and Kieno F, *Journal of Applied Sciences*, **2009**, 19, 3424.
[3] Kam S, Zerbo L, Bathiebo DJ, SoroJ, Naba S, Wenmenga U, Traoré K, Gomina M, Blanchart P, Permeability to water of sintered clay ceramics. *Applied Clay Science*, **2009**, 46, 4, 351.
[4] Chauhan J and Yadav P, *Der Pharmacia Sinica*, **2011**, 2, 228.
[5] Srilatha G, Thilagavathi B and Varadharajan D, *Advances in Applied Science Research*, **2012**, 3, 201.
[6] Morgan PR, Yerazunis S, *Rensselaer Polytechnic Institute, Troy, AICHE*, Wiley Inter-Science publication, New York **1967**.
[7] Kondjoyan A, Daudin JD, *International Journal of Heat and Mass Transfer*, **1993**, 36, 1807.
[8] Prabal T, Conrad RI, . Carey JS, *International Journal of Heat and Mass Transfer*, **2008**, 51, 3091.
[9] Conrad RI, . Carey JS, *International Journal of Heat and Mass Transfer*, **2007**, 50, 2376.
[10] Berman LD - *Evaporative cooling of circulating water*, Pergamon Press, **1961**.
[11] C.T.T.B. -*Tuiles et briques de terre cuite - Caractéristiques et mise en œuvre, Essai d'imperméabilité ;* NF EN 539-1 Editeur: Le Moniteur, Collection : Mémento technique, 1ère édition, **1998**.
[12] Perrin BL, Wardeh G, Poeydemenge F. *L'Industrie céramique & verrière*, **2004**, 992, 30.
[13] Bejan A, C*onvection heat transfer*, A Wiley-Interscience Publication, 2nd Edition, **1995**.
[14] Kishan N and Maripala S, *Advances in Applied Science Research*, **2012**, 3, 60.
[15] Rami Reddy G and Venkataramana S, *Advances in Applied Science Research*, **2011,** 2, 240.
[16] Gilliland ER and Sherwood TK. - *Ind. Eng. Chem.*, **1934**, 26, 516.
[17] A.P. Colburn, *Trans. AICHE*, **1933**, 29, 174.
[18] Prerna P. Dhawade and Ramanand N. Jagtap, *Advances in Applied Science Research*, **2012**, 3 1372.